Electronic Supplementary Material (ESI) for Physical Chemistry Chemical Physics.

Supporting Information

Fluorescence Band Exchange Narrowing in a Series of Squaraine Oligomers: Energetic vs. Structural Disorder

Arthur Turkin,[a] Pavel Malý,[b] Christoph Lambert,[a,c*]

[a]Institut für Organische Chemie, Universität Würzburg, Am Hubland, D-97074 Würzburg, Germany.

[b]Institut für Physikalische und Theoretische Chemie, Universität Würzburg, Am Hubland, D-97074 Würzburg, Germany.

[c]Center for Nanosystems Chemistry, Universität Würzburg, Theodor-Boveri-Weg, D-97074 Würzburg, Germany

Table of Contents

1 Materials and Methods 1
2 Fluorescence Spectroscopy 3
3 Calculations 12
4 References 13

1 Materials and Methods

Steady-State Absorption Spectroscopy

- Jasco V670 UV/vis/NIR spectrophotometer (software: SpectraManager v.2.08.04)
- Agilent Technologies Cary 5000 UV/vis/NIR spectrophotometer (software: Agilent Cary WinUV Analysis and Bio v.4.2)

Spectroscopic grade solvents were used as received (Acros Organics, Supelco, VWR). Absorption measurements were carried out in silylated quartz cuvettes from Starna (10 mm, Pfungstadt, Germany) at r.t. Silylation procedure was carried out according to literature. Aggregation of oligomers could be excluded by measuring a series of samples with different concentrations (10^{-7} – 10^{-5}). Transition dipole moments were calculated with Eq. S1:

$$\mu_{eg}^2 = \frac{3hc\varepsilon_0 \ln(10) 9n}{2000\pi^2 N_{Av}(n^2+2)^2} \int \frac{\varepsilon}{\tilde{\nu}} d\tilde{\nu} \qquad \text{S1}$$

where h is the Planck constant, c is the speed of light (3×10^{10} cm s^{-1}), ε_0 is the electric field constant, n is the refractive index of the solvent, N_{Av} is the Avogadro constant and $\varepsilon(\tilde{\nu})$ is the extinction coefficient as a function of the wavenumber $\tilde{\nu}$.

Steady-State Emission Spectroscopy

Edinburgh Instruments FLS980 fluorescence lifetime spectrometer

- Software F980 v.1.4.5
- 450 W continuous xenon arc lamp
- Double excitation and emission monochromator
- PMT (R5509-42)

Steady-state emission spectra were recorded at r.t. in silylated 10 mm quartz cells from Starna (Pfungstadt, Germany). All solvents were of spectroscopic grade and were used as received. Emission and excitation scans were performed on strongly diluted samples (OD < 0.05) in order to prevent self-absorption. Emission spectra were corrected ($I_{fl} \times \lambda^2$) before normalizing. Fluorescence quantum yields were determined using optical dense samples in an integrating sphere and Eq. S2:

$$\Phi_{obs} = \frac{\int F_{sample}}{\int E_{solvent} - \int E_{sample}} \qquad \text{S2}$$

where Φ_{obs} is the observed quantum yield, F_{sample} is the fluorescence emission spectrum of the sample, E_{sample} is the spectrum of the light used to excite the sample and $E_{solvent}$ is the spectrum of the light used for excitation with a blank sample. The observed fluorescence quantum yields were corrected for self-absorption by means of the method of Bardeen at al., using Eq. S3:

$$1 - a = \frac{\int_0^\infty F_{fl}(\lambda) d\lambda}{\int_0^\infty F_{emission}(\lambda) d\lambda} \qquad \text{S3}$$

Where a is the probability of self-absorption of an emitted photon, thus $1 - a$ is the escape probability, and the fluorescence spectrum of a diluted sample F_{fl} (OD < 0.05) is compared to an

optical dense sample $F_{emission}$. Using Eq. S3 the quantum yield Φ_{fl} of the sample can be determined:

$$\Phi_{fl} = \frac{\Phi_{obs}}{1 - a + a\Phi_{obs}} \qquad \text{S4}$$

Excitation spectra were recorded with the same setup.

Time Dependent Fluorescence-Emission

Edinburgh Instruments FLS980 fluorescence lifetime spectrometer

- Pulsed laser diode (PLD): 15250 nm^{-1} (656 nm)
- PMT (H10720-01)
- Software: FAST v.3.4.2

Fluorescence lifetimes were determined by time-correlated single photon counting (TCSPC). The samples were prepared similar to the steady-state emission experiments (*OD* < 0.04) and measured under magic angle conditions. The instrument response function (IRF) was determined using a scatterer solution consisting of colloidal silica (LUDOX) in deionised water. Lifetimes were determined by deconvolution of the experimental decay with the IRF. The decay was fitted with exponential decay functions.

2 Fluorescence Spectroscopy

Table S1 Summary of spectroscopic data of the squaraine oligomer series.

		$\tilde{\nu}_{abs}$ / cm^{-1} (nm)	μ_{eg} / D^2	$\tilde{\nu}_{em}$ / cm^{-1} (nm)	*Stokes* shift / cm^{-1}	Φ_{fl} / –	τ_{fl}^{d} / ns
SQ	$CHCl_3$	14600 (685)	103	14200 (702)[a]	300	0.55	2.52
	acetone	14700 (681)	115	14300 (698)[b]	400	0.20	0.94
SQ_2	$CHCl_3$	13600 (735)	233	13300 (751)[c]	300	0.27	1.01
	acetone	13700 (732)	260	–	–	–	–
SQ_3	$CHCl_3$	13100 (761)	363	12900 (776)[c]	300	0.27	1.07 (0.87) 1.58 (0.13)[e]
	acetone	13200 (759)	336	–	–	–	–
SQ_4	$CHCl_3$	12900 (773)	480	12700 (785)[c]	200	0.29	1.07
	acetone	13000 (771)	536	–	–	–	–
SQ_5	$CHCl_3$	12800 (780)	636	12600 (791)[c]	200	0.30	1.11
	acetone	15000 (666)	680	–	–	–	–
SQ_6	$CHCl_3$	12800 (784)	738	12600 (794)[c]	200	0.32	1.13
	acetone	15300 (656)	757	–	–	–	–
SQ_7	$CHCl_3$	12700 (785)	912	12600 (794)[c]	200	0.30	1.05
	acetone	15400 (648)	906	–	–	–	–
SQ_8	$CHCl_3$	12700 (785)	1037	12500 (798)[c]	200	0.33	1.08
	acetone	15500 (644)	995	–	–	–	–
SQ_9	$CHCl_3$	12700 (785)	1158	12500 (798)[c]	200	0.39	1.17
	acetone	15500 (644)	1123	–	–	–	–

Excitation at [a]15400 cm^{-1} (650 nm), [b]15900 cm^{-1} (630 nm) and [c]15200 cm^{-1} (660 nm). [d]Multiexponential decay

measured by TCSPC, excitation at 15200 cm^{-1} (656 nm), amplitudes are given in brackets. [e]Amplitude average lifetime: 1.14 ns.

a)

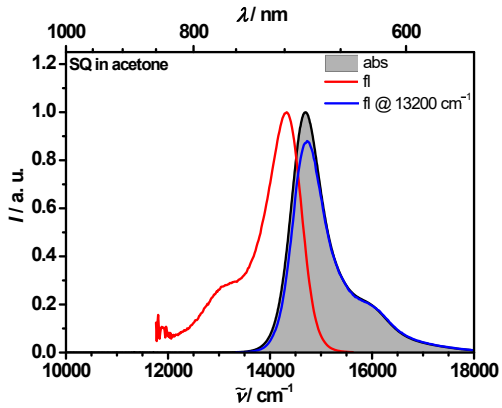
λ/ nm
1000
800
600
SQ in acetone
abs
fl
fl @ 13200 cm-1
I / a. u.
1.2
1.0
0.8
0.6
0.4
0.2
0.0
10000
12000
14000
16000
18000
ν̃/ cm-1

b)

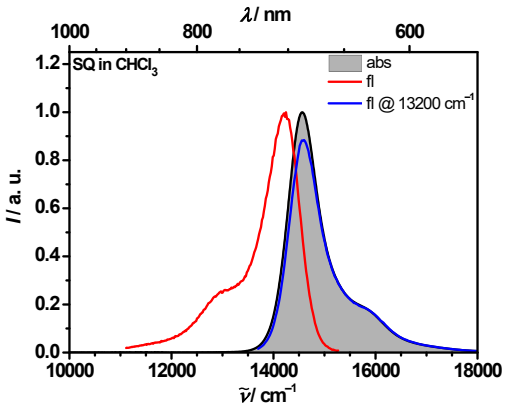
λ/ nm
1000
800
600
SQ in CHCl3
abs
fl
fl @ 13200 cm-1
I / a. u.
1.2
1.0
0.8
0.6
0.4
0.2
0.0
10000
12000
14000
16000
18000
ν̃/ cm-1

c)

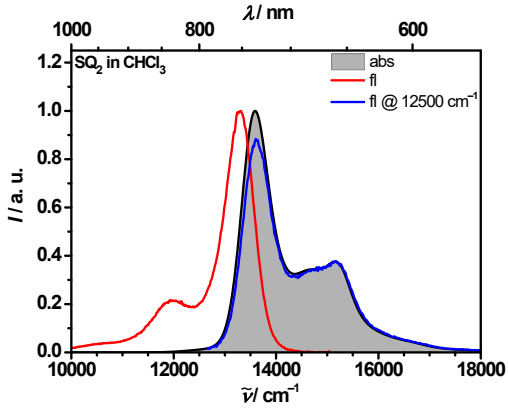
λ/ nm
1000
800
600
SQ2 in CHCl3
abs
fl
fl @ 12500 cm-1
I / a. u.
1.2
1.0
0.8
0.6
0.4
0.2
0.0
10000
12000
14000
16000
18000
ν̃/ cm-1

d)

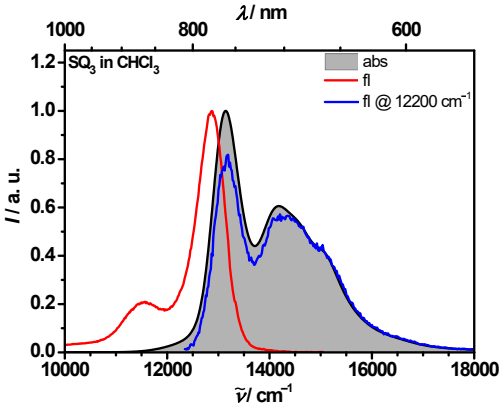
λ/ nm
1000
800
600
SQ3 in CHCl3
abs
fl
fl @ 12200 cm-1
I / a. u.
1.2
1.0
0.8
0.6
0.4
0.2
0.0
10000
12000
14000
16000
18000
ν̃/ cm-1

e)

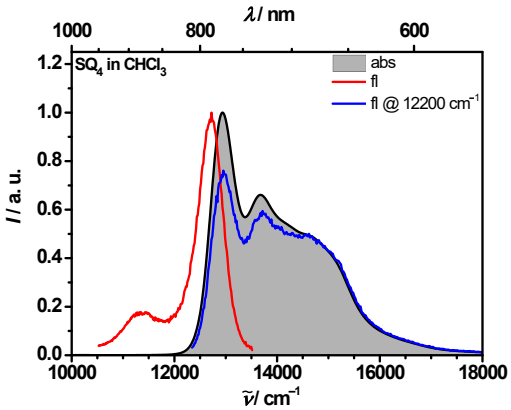
λ/ nm
1000
800
600
SQ4 in CHCl3
abs
fl
fl @ 12200 cm-1
I / a. u.
1.2
1.0
0.8
0.6
0.4
0.2
0.0
10000
12000
14000
16000
18000
ν̃/ cm-1

f)

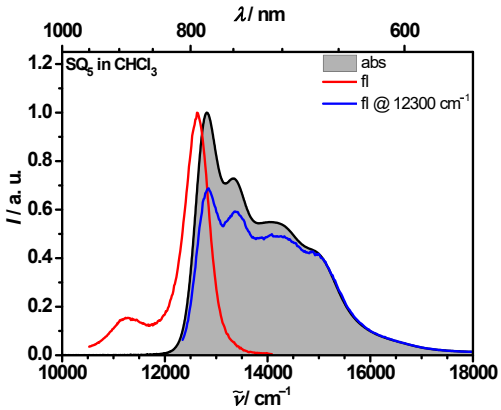
λ/ nm
1000
800
600
SQ5 in CHCl3
abs
fl
fl @ 12300 cm-1
I / a. u.
1.2
1.0
0.8
0.6
0.4
0.2
0.0
10000
12000
14000
16000
18000
ν̃/ cm-1

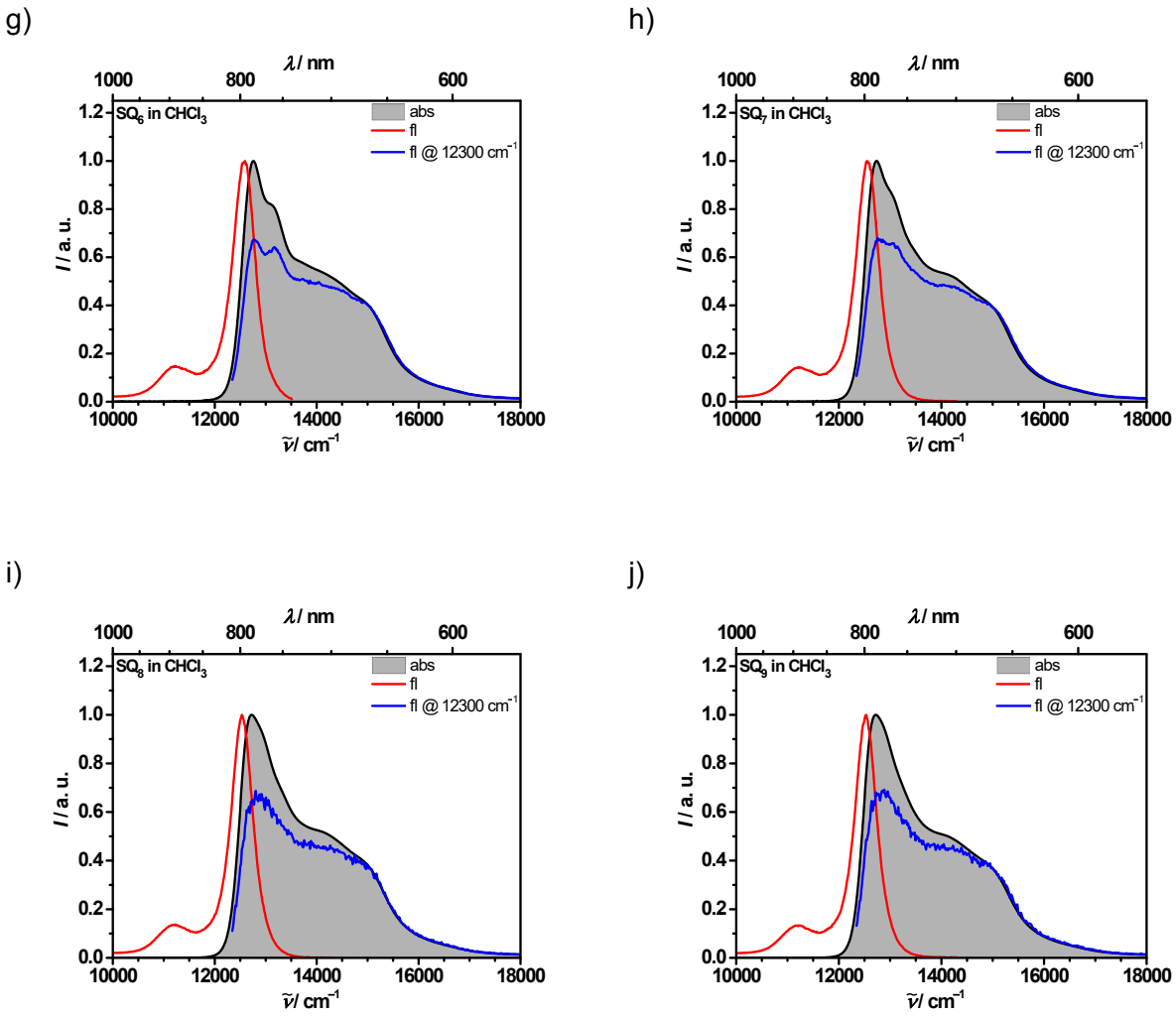

Fig. S1 Normalised absorption (grey shaded), emission (red solid line) and excitation (blue solid line) spectra of the oligomers in (a) acetone and (b-j) $CHCl_3$. Even though a low concentration was used for emission experiments (*OD* < 0.04) deviations in the excitation spectra at lower energy are clearly visible. This issue is due to an inner filter effect, see Fig. S2.

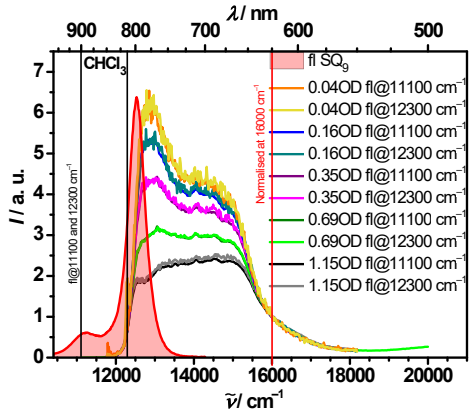

Fig. S2 Emission (red) and excitation spectra at various concentrations of **SQ_9** in $CHCl_3$. The spectra were measured at two emission wavelengths, 12300 and 11100 cm^{-1}, respectively, and were normalised at 16000 cm^{-1}.

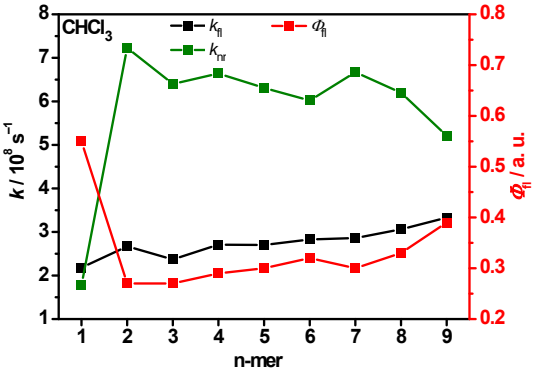

Fig. S3 Comparison of radiative rate constant k_{fl}, non-radiative rate constant k_{nr} and quantum yield Φ_{fl} in $CHCl_3$.

Table S2 Summary of rate constants and quantum yields.

	k_{fl}[a] / × 10^8 s^{-1}	k_{nr}[b] / × 10^8 s^{-1}	Φ_{fl} / –
SQ	2.18	1.78	0.55
SQ$_2$	2.67	7.23	0.27
SQ$_3$	2.37	6.40	0.27
SQ$_4$	2.71	6.64	0.29
SQ$_5$	2.70	6.31	0.30
SQ$_6$	2.83	6.02	0.32
SQ$_7$	2.86	6.67	0.30
SQ$_8$	3.06	6.20	0.33
SQ$_9$	3.33	5.21	0.39

[a]k_{fl} is the radiative rate constante $k_{fl} = \frac{\Phi_{fl}}{\tau_{fl}}$ and [b]k_{nr} is the non-radiative rate constante $k_{nr} = \frac{1}{\tau_{fl}} - k_{fl}$.

Comparison of Transition Dipole Moments

Fluorescence transition dipole moments (μ_{fl}) calculated via the Strickler-Berg equation (S4):

$$k_{fl} = \frac{16 \times 10^6 \pi^3 n(n^2+2)^2}{3h\varepsilon_0 \quad 9} \langle \tilde{\nu}_{fl}^{-3} \rangle \mu_{fl}^2 \qquad \text{S4}$$

where h is the Planck constant, ε_0 is the vacuum permittivity, n is the refractive index (n_{CHCl3} = 1.4459, $n_{toluene}$ = 1.4969), and the averaged cubic fluorescence energy:

$$\langle \tilde{\nu}_{fl}^{-3} \rangle_{av}^{-1} = \frac{\int I_{fl} d\tilde{\nu}}{\int \tilde{\nu}^{-3} I_{fl} d\tilde{\nu}} \qquad \text{S5}$$

with $I_{fl} = I_\lambda \times \lambda^2$

Table S3 Collection of absorption and fluorescence transition dipole moment data.

	μ_{eg}^2 / D²	μ_{fl}^2 / D²	μ_{S1a}^2 / D²
SQ	103	98.0	114
SQ$_2$	233	146	178
SQ$_3$	363	143	200
SQ$_4$	480	168	214
SQ$_5$	636	168	267
SQ$_6$	738	180	298
SQ$_7$	912	183	366
SQ$_8$	1037	196	399
SQ$_9$	1158	214	454

[a]From Fig. S4.

μ_{S1}^2 was determined by fitting the mirror image of the fluorescence spectra plotted as $I/\tilde{\nu}^3$ to the low energy side of the absorption spectra (plotted as $I/\tilde{\nu}$). This yields a rough estimation for the band shape and intensity of the lowest energy exciton absorption band S_1 and allows to calculate the transition dipole moment μ_{S1}^2 by integration using Eq. S1.

a)

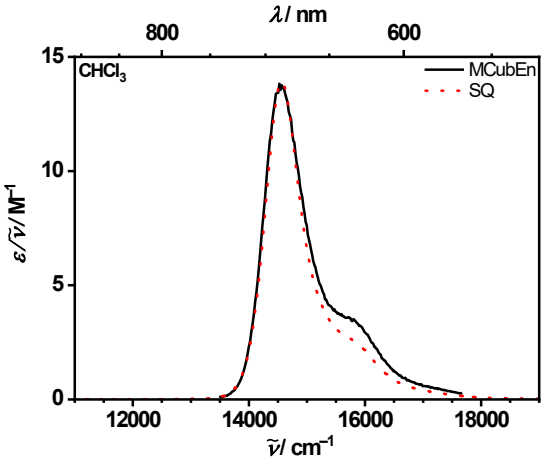
λ/ nm
800
600
CHCl3
MCubEn
SQ
ε/ν̃/ M-1
ν̃/ cm-1
0
5
10
15
12000
14000
16000
18000

b)

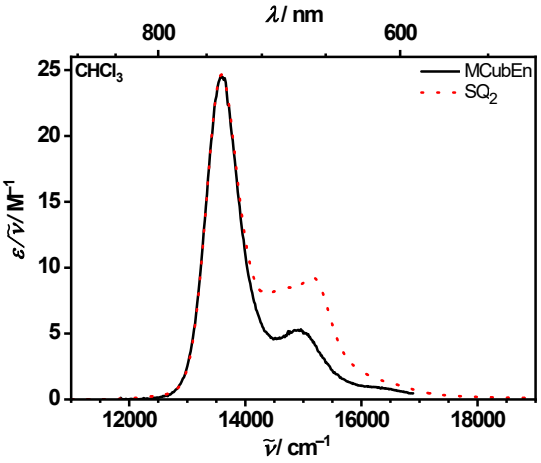
λ/ nm
800
600
CHCl3
MCubEn
SQ2
ε/ν̃/ M-1
ν̃/ cm-1
0
5
10
15
20
25
12000
14000
16000
18000

c)

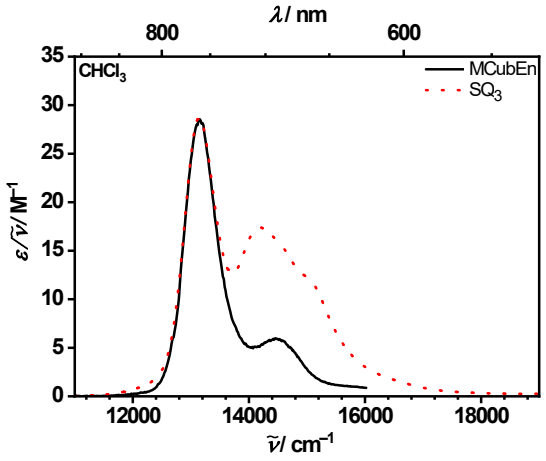
λ/ nm
800
600
CHCl3
MCubEn
SQ3
ε/ν̃/ M-1
ν̃/ cm-1
0
5
10
15
20
25
30
35
12000
14000
16000
18000

d)

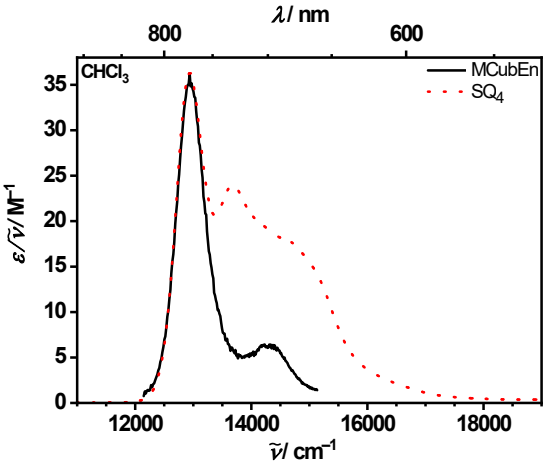
λ/ nm
800
600
CHCl3
MCubEn
SQ4
ε/ν̃/ M-1
ν̃/ cm-1
0
5
10
15
20
25
30
35
12000
14000
16000
18000

e)

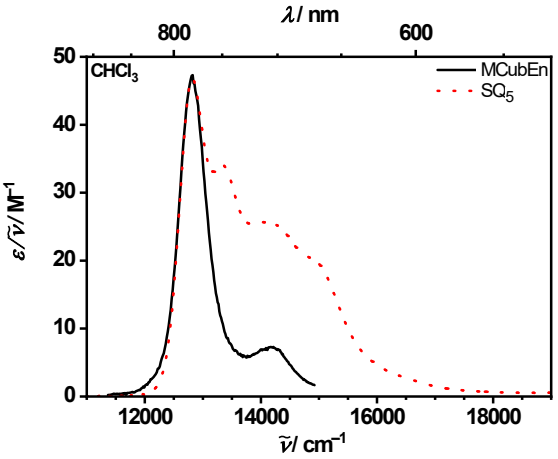
λ/ nm
800
600
CHCl3
MCubEn
SQ5
ε/ν̃/ M-1
ν̃/ cm-1
0
10
20
30
40
50
12000
14000
16000
18000

f)

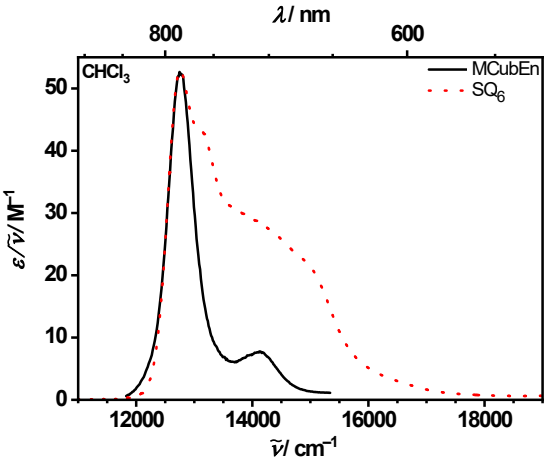
λ/ nm
800
600
CHCl3
MCubEn
SQ6
ε/ν̃/ M-1
ν̃/ cm-1
0
10
20
30
40
50
12000
14000
16000
18000

g)

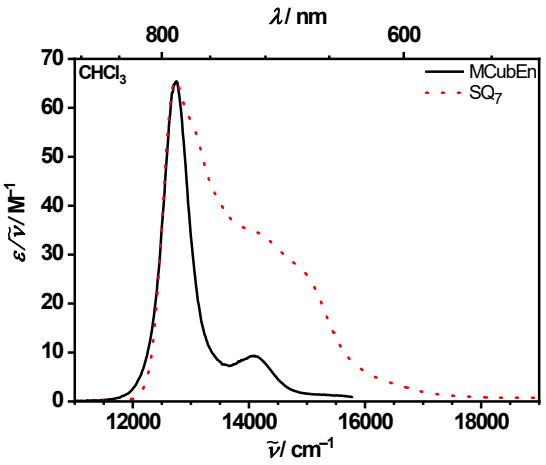

h)

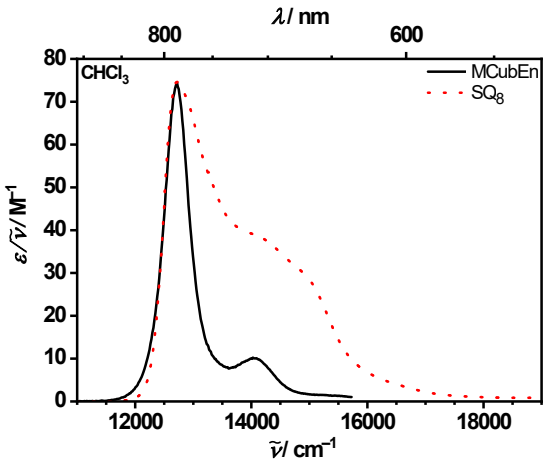

i)

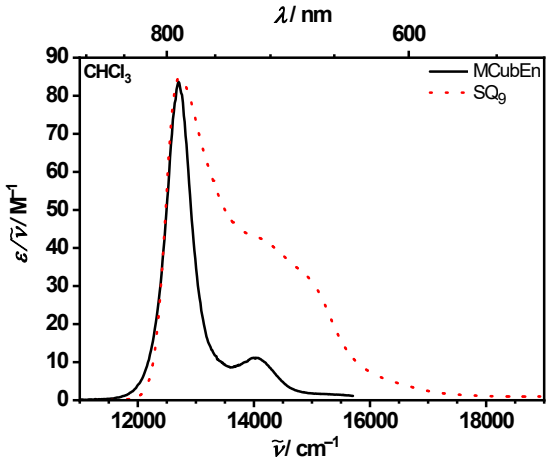

Fig. S4 Absorption spectra (dashed red line, $I/\tilde{\nu}$.) in $CHCl_3$ plotted next to the mirrored fluorescence spectra ("MCubEn", solid black line, $I/\tilde{\nu}^3$).

Table S4 Determined coherence length of both experimental and calculated data.

	$N_{coh} = S_{HR}\frac{I_{00}}{I_{01}}$		$N_{coh} = \left(\frac{fwhm_{SQ}}{fwhm_{SQ_n}}\right)^2$		$N_{coh} = \frac{\mu_{fl}^2(SQ_n)}{\mu_{fl}^2(SQ)}$	**Direct** N_{coh}
	Exp.	**Calc.**	**Exp.**	**Calc.**	**Exp.**	**Calc.**
SQ	1.00	1.00	1.00	1.00	1.00	1.00
SQ_2	1.39	1.72	1.41	1.54	1.49	1.79
SQ_3	1.45	2.20	1.45	1.93	1.46	2.04
SQ_4	2.06	2.55	1.85	2.16	1.71	2.41
SQ_5	2.11	2.77	2.07	2.34	1.71	2.60
SQ_6	2.37	2.84	2.29	2.39	1.84	2.80
SQ_7	2.22	2.95	2.34	2.55	1.87	2.94
SQ_8	2.23	2.91	2.53	2.49	2.00	3.06
SQ_9	2.29	2.91	2.43	2.55	2.18	3.16

3 Calculations

Table S5 Values used for the excitonic model.

Quantity	Value	Quantity	Value
Transition energy	$e_B = 14670\ cm^{-1}$	Helix pitch	$2\ nm$
Reorganisation energy	$\lambda_c = 240\ cm^{-1}$	Energetic disorder (st. deviation)	$\sigma = 260\ cm^{-1}$
Bath parameters (Eq. 4 of the main text)	$\Lambda = 600\ cm^{-1}$, $\Omega = 1200\ cm^{-1}$, $S_{HR} = 0.22$, $\gamma = 30\ cm^{-1}$	Linear orientation disorder (st. deviation)	$\sigma = 50°$
Averaging	100000x	Helical rise angle disorder (st. deviation)	$\sigma = 15°$
Linear chain angle	$\theta_{lin} = 0°$	Helical azimutal angle disorder (st. deviation)	$\sigma = 0°$
SQ arc angle	$\theta_{arc} = 140°$	SQ length	$1.5\ nm$

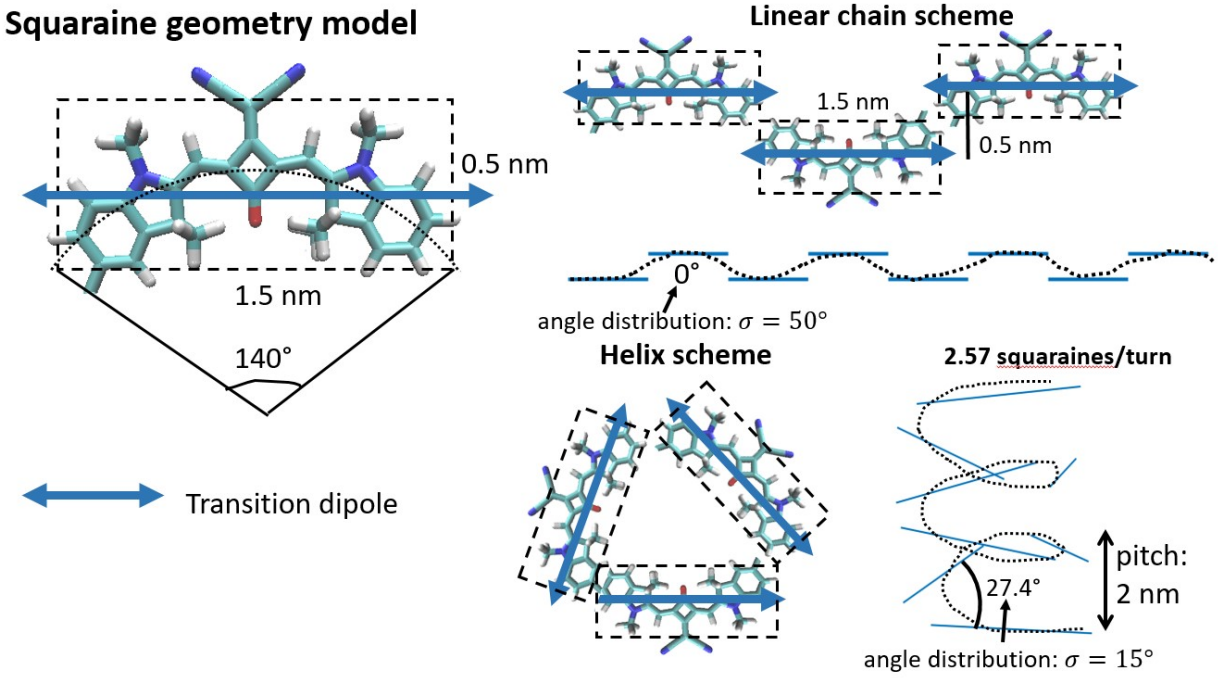

Fig. S5 Squaraine coil and helix geometry used for the calculations.

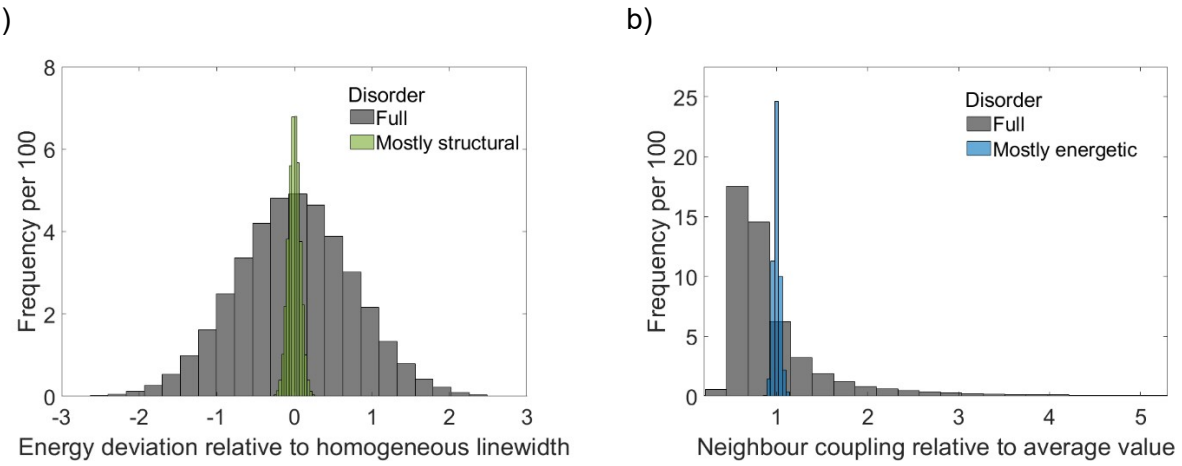

Fig. S6 Extent of diagonal and off-diagonal disorder. (a) Distribution of energetic deviations from the mean value, relative to the homogeneous linewidth (347 cm^{-1}). Black: full energetic disorder, green: reduced to 10% (i.e., remaining disorder is mostly structural). (b) Distribution of nearest-neighbour coupling in the linear geometry, relative to the mean value (−515 cm^{-1}). Black: full structural disorder, blue: reduced to 10% (i.e., remaining disorder is mostly energetic).

4 References

1. G. A. Olah, S. C. Narang, B. G. B. Gupta and R. Malhotra, *J. Org. Chem.* 1979, **44**, 1247.
2. T.-S. Ahn, R. O. Al-Kaysi, A. M. Müller, K. M. Wentz and C. J. Bardeen, *Rev. Sci. Instrum.* 2007, **78**, 086105.
3. S. Kumar Panigrahi and A. Kumar Mishra, *JPPC* 2019, **41**, 100318.